



Cite this: *Chem. Commun.*, 2016, 52, 5734

Received 22nd February 2016,  
Accepted 21st March 2016

DOI: 10.1039/c6cc01597b

www.rsc.org/chemcomm

## Rational synthesis of an exceptionally stable Zn(II) metal–organic framework for the highly selective and sensitive detection of picric acid†

Yingli Hu,<sup>‡a</sup> Meili Ding,<sup>‡a</sup> Xiao-Qin Liu,<sup>b</sup> Lin-Bing Sun<sup>b</sup> and Hai-Long Jiang<sup>\*ab</sup>

**Based on an organic ligand involving both carboxylate and tetrazole groups, a chemically stable Zn(II) metal–organic framework has been rationally synthesized and behaves as a fluorescence chemosensor for the highly selective and sensitive detection of picric acid, an extremely hazardous and strong explosive.**

Metal–organic frameworks (MOFs), also called porous coordination polymers (PCPs), have become a class of sought-after porous materials over the past two decades, not only due to their great structural tailorability, diversity, as well as extremely high surface area and porosity, but also because of their potential applications in various domains, such as gas storage and separation, sensing, catalysis and drug delivery.<sup>1–4</sup> Despite this, stability has been recognized to be one of the most important obstacles on the way to practical applications of MOFs. Generally, MOFs remain stable up to 250 °C, an acceptable temperature as porous functional materials. However, most MOFs are sensitive to moisture/water, and it remains rare for MOFs that are survived in acidic or basic media.<sup>5</sup> The origin of unstable MOFs should be caused by the low bond energy of the coordination bond based on the Hard-Soft-Acid-Base theory (HSAB). The soft-acid metal cations (such as Zn<sup>2+</sup> and Cu<sup>2+</sup>) would coordinate with soft-base N donor ligands, forming much stronger metal–N bonds than those of metal–O bonds by coordination with the hard-base carboxylate ligands. However, the stronger is the coordination bond between the metal ion and the ligand, the poorer is the crystallinity and the smaller the crystals for

the resultant MOFs. Then it is very hard to obtain good crystals large enough for structural characterization with single crystal X-ray diffraction. Taking both the factors together, the crystallinity and stability of MOFs seem to be contradictory factors; the rational selection of metal ions and ligands in the synthesis of MOFs would be of great importance to afford MOFs with good stability and good single crystals.

On the other hand, the sensitive and selective detection of nitro-explosives is drawing enormous attention due to their broad applications in many fields.<sup>6</sup> Among the common nitro-explosives, picric acid (PA, also called 2,4,6-trinitrophenol (TNP)) is an extremely hazardous and strong explosive, and the contamination of PA in ground water/soil causes severe health problems.<sup>7</sup> Hence, the facile and selective detection of PA is in high demand, while relatively rare reports can be found on this.<sup>8</sup> Fluorescence chemosensors, especially MOF-based sensors, have been recently demonstrated to be very promising for the detection of nitro-explosives owing to their high sensitivity and convenient visual detection, as well as the merits of MOFs mentioned above.<sup>6,9</sup> Bearing the aforementioned points in mind, the construction of MOFs based on electron rich  $\pi$ -conjugated ligands would afford a fluorescence sensor for the detection of nitro-explosives like PA, and the chemical stability of the MOF sensors would guarantee their application in real world.

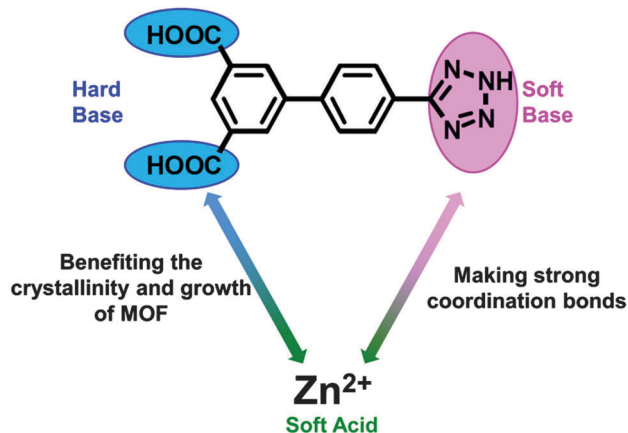
In this work, on the basis of a  $\pi$ -conjugated ligand, 4'-(1H-tetrazol-5-yl)-[1,1'-biphenyl]-3,5-dicarboxylic acid (H<sub>3</sub>TZBPDC), involving both soft-base and hard-base coordination sites (tetrazole and carboxylic acid, respectively), a soft acid (Zn<sup>2+</sup>)-based MOF, Zn<sub>2</sub>(TZBPDC)( $\mu_3$ -OH)(H<sub>2</sub>O)<sub>2</sub> (denoted as **USTC-7**), with exceptional chemical stability that maintains framework integrity not only in diverse boiling solvents but also in the aqueous solutions with pH ranging from 2 to 12, has been rationally synthesized (Scheme 1). The strong coordination bonds between Zn(II) ions and nitrogen sites of tetrazole would enable the high stability of the resultant MOF, while the relatively weak coordination between the Zn(II) ion and oxygen from carboxylate benefits the growth of big single crystals for structural characterization. There have been very limited reports on the stable MOFs that are sustainable in both acidic and

<sup>a</sup> Hefei National Laboratory for Physical Sciences at the Microscale, CAS Key Laboratory of Soft Matter Chemistry, Collaborative Innovation Center of Suzhou Nano Science and Technology, Department of Chemistry, University of Science and Technology of China, Hefei, Anhui 230026, P. R. China. E-mail: jianglab@ustc.edu.cn

<sup>b</sup> State Key Laboratory of Materials-Oriented Chemical Engineering, College of Chemistry and Chemical Engineering, Nanjing Tech University, Nanjing 210009, China

† Electronic supplementary information (ESI) available: Experimental procedures, crystallographic data of **USTC-7**, TG plot and figures referred in the text. CCDC 1455029. For ESI and crystallographic data in CIF or other electronic format see DOI: 10.1039/c6cc01597b

‡ These authors contributed equally to this work.



Scheme 1 Illustration of the rational design of stable MOFs based on Zn(II) ions and the ligand involving carboxylate and tetrazole groups.

basic solutions with a wide pH range.<sup>10</sup> To the best of our knowledge, this is among the broadest pH range that a Zn-carboxylate MOF can survive thus far. It is believed that the Zn–N bonds play a central role in the stability. Remarkably, thanks to the  $\pi$ -electron-rich entity of the ligand, **USTC-7** exhibits strong fluorescence and displays the selective fluorescence sensing of a trace amount of PA.

Single crystals of **USTC-7** with high quality were obtained by the solvothermal reaction of H<sub>3</sub>TZBPDC and Zn(NO<sub>3</sub>)<sub>2</sub>·6H<sub>2</sub>O in a DMF/H<sub>2</sub>O/DMSO mixed solvent at 85 °C for 3 days. Single crystal X-ray diffraction analysis reveals that **USTC-7** crystallizes in an orthorhombic system with a space group of *Cmcm*. The asymmetric unit contains two crystallographically unique Zn(II) ions and a half TZBPDC ligand, all of which are located on a 2-fold axis and a mirror in the same occupancy of 1/4. The Zn(1) is pseudo-octahedrally coordinated by two nitrogen atoms from two ligands at the axial position, two oxygen atoms from  $\mu_3$ -OH groups and the other two oxygen atoms from coordinated water molecules making up the basal plane (Fig. 1a). The Zn(2) is coordinated by two nitrogen atoms from two ligands in the axial direction while three oxygen atoms from one  $\mu_3$ -OH group and two coordinated water molecules in the plane to construct a trigonal bipyramidal environment (Fig. 1a). The Zn(1)–N bond distance of 2.111(4) Å is much shorter than that of the Zn(2)–N bond of 2.385(4) Å, both of which are comparable to the reported distance values.<sup>11a</sup> Inversely, the Zn(1)–O bond distances, falling in the range of 2.110(3)–2.159(7) Å, are slightly longer than Zn(2)–O bond lengths of 1.983(5) Å and 2.035(6) Å, all of which are within normal ranges.<sup>11b</sup> The TZBPDC ligand bridges to six Zn(II) ions, in which each nitrogen and each carboxylate bridge to one Zn(II) ion (Fig. 1a). The  $\mu_3$ -OH connects to two Zn(1) and one Zn(2) centers (Fig. 1a). In this binding fashion, the Zn(II) ions are bridged by  $\mu_3$ -OH groups and TZBPDC ligands to afford a 3D network involving slabs of 6.9 Å width constructed by Zn–N and  $\mu_3$ -OH–Zn bonds (Fig. 1b and c). There are two types of channels with sizes of around 5.9 and 2.5 Å, respectively, in **USTC-7** and the large ones, composed of two slabs and benzene carboxylic acids, are highlighted by the yellow tubes (Fig. 1b and c). The effective free volume is ~30%, as calculated using PLATON.<sup>12</sup> The CO<sub>2</sub> sorption for **USTC-7** has been measured at 195 K and

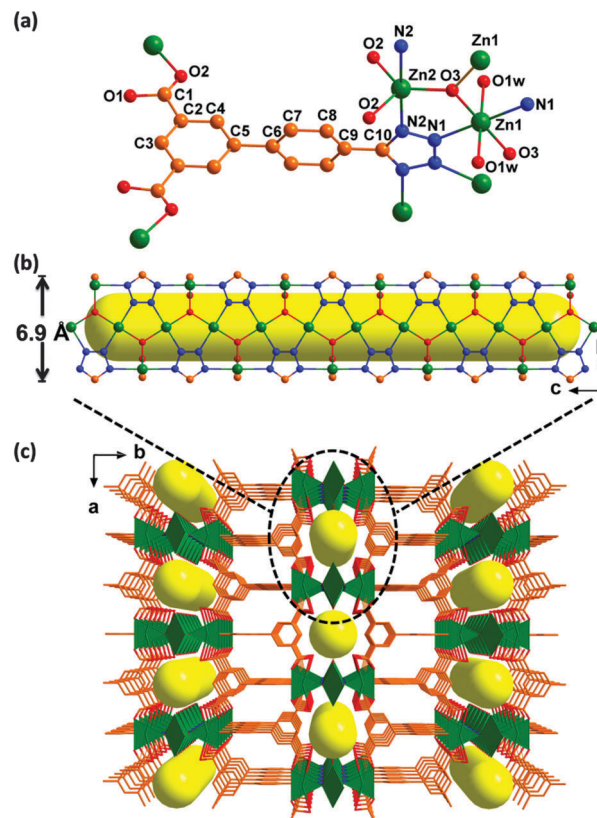


Fig. 1 (a) The coordination environment of Zn(II) ions, the  $\mu_3$ -OH group and the TZBPDC ligand in **USTC-7**; (b) the large channel highlighted with a yellow tube constructed by benzene carboxylic acids and two slabs (one is shown and the other is shaded by the tube) involving Zn–N and  $\mu_3$ -OH–Zn bonds; (c) view of the 3D network of **USTC-7**. The ZnO<sub>3</sub> and ZnO<sub>4</sub> polyhedra are shaded in olive green for clarity.

exhibits a type I isotherm (Fig. S3, ESI<sup>†</sup>), indicating that **USTC-7** is a microporous material with a pore volume of 0.17 cm<sup>3</sup> g<sup>−1</sup> and the BET surface area of 230 m<sup>2</sup> g<sup>−1</sup>.<sup>13</sup>

To our delight, the single crystals of **USTC-7** remain unchanged in air for a very long time as expected. To further investigate the stability of **USTC-7**, it was soaked in aqueous solutions with different pH values and a variety of boiling organic solvents. Powder X-ray diffraction (XRD) patterns have unambiguously demonstrated that the crystallinity and framework integrity of **USTC-7** can be well retained in not only diverse boiling solvents (ethanol, ethyl acetate, toluene, hexane) for 12 h but also pH = 2–12 aqueous solutions (Fig. 2), setting **USTC-7** among the most stable MOFs that is tolerable in wide pH ranges as far as possible.<sup>10</sup> Particularly, **USTC-7** remains unchanged in water for over 4 months (Fig. 2b). So far, almost all reported Zn-carboxylate MOFs are more or less sensitive to moisture/water. It is believed that the exceptional stability of **USTC-7** is attributed to the strong Zn–tetrazole N bonds as predesigned. Undoubtedly, the great stability of **USTC-7** guarantees its retained structure during the functional study and thus builds a nice basis for its further application.

Taking into account the excellent luminescence properties of MOFs composed of d<sup>10</sup> metal centers and/or electron-rich  $\pi$ -conjugated ligands,<sup>14</sup> the fluorescence of both **USTC-7** and

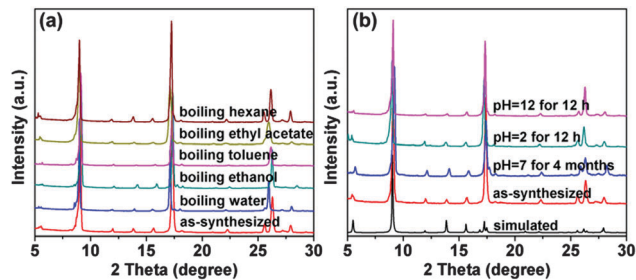


Fig. 2 Powder XRD profiles of **USTC-7** (a) after being soaked in various boiling solvents for 12 h; (b) after being soaked in water, acidic and basic solutions for different time lengths.

the  $H_3$ TZBPDC ligand was investigated in the solid state. It can be observed that a strong emission of **USTC-7** occurs at around 370 nm while a weak emission of the  $H_3$ TZBPDC ligand occurs at 409 nm under  $\lambda_{ex} = 309$  nm (Fig. S5 and S6, ESI<sup>†</sup>). The emission band for **USTC-7** could be tentatively attributed to the ligand-to-metal charge transfer (LMCT).<sup>14</sup> The remarkable fluorescence and stability of **USTC-7** encourage us to investigate its potential for the fluorescence sensing of nitro-explosives in various solvents. The stable suspension of **USTC-7** in different solvents, including  $H_2O$ , DMF,  $CHCl_3$ ,  $C_2H_5OH$  and  $CH_3CN$ , was examined and the  $CHCl_3$  suspension showed the highest intensity with two peaks at 408 and 432 nm, totally different from those in other solvents (Fig. S7, ESI<sup>†</sup>). Hence, the  $CHCl_3$  suspension of **USTC-7** was chosen to detect different kinds of nitro-explosives including picric acid (PA), 2,4-dinitrotoluene (2,4-DNT), 2,6-dinitrotoluene (2,6-DNT), 2,4,6-trinitrotoluene (TNT), nitrobenzene (NB) and *m*-dinitrobenzene (*m*-DNB). As displayed in Fig. 3a, the fluorescence intensity decreases steadily along with the increase of PA concentration. Upon introducing only 20  $\mu$ L of PA, the fluorescence intensity of **USTC-7** lowers to 16.6% of the original value (Fig. 3a). This photoluminescence quenching result is comparable to or even better than that for previously reported MOF sensors used for PA detection.<sup>8</sup> In sharp contrast, all other nitro-explosives show little or no effect on the fluorescence of **USTC-7** (Fig. S8–S12, ESI<sup>†</sup>). The results demonstrate that **USTC-7** has high selectivity for PA among diverse nitro-explosives (Fig. 3b and c). The fluorescence quenching efficiency can be quantitatively explained using the Stern–Volmer (SV) equation:  $(I_0/I) = 1 + K_{sv}[Q]$ , in which  $K_{sv}$  is the quenching constant ( $M^{-1}$ ),  $[Q]$  is the molar concentration of the analyte (mM),  $I_0$  and  $I$  are the fluorescence intensities before and after the addition of the analyte, respectively. The Stern–Volmer plots for PA are nearly linear at low concentrations ( $R^2 = 0.9989$ ) with the  $K_{sv}$  value of  $4.90 \times 10^4 M^{-1}$ , which is among the highest values for MOF-based PA sensors (Fig. 3d).<sup>8</sup> The standard deviation of this detection method and the PA detection limit are calculated to be 7.36 and  $2.78 \times 10^{-4}$  mM, respectively (Fig. S13 and Tables S3, S4, ESI<sup>†</sup>). The low detection concentration and the high quenching constant for PA reveal that **USTC-7** is an excellent sensor for the sensitive and selective detection of PA. Moreover, the structural integrity of **USTC-7** has been unambiguously demonstrated after fluorescence sensing (Fig. S14, ESI<sup>†</sup>).

To further verify the highly selective sensing behavior of **USTC-7** towards PA, some competitive experiments were performed by the

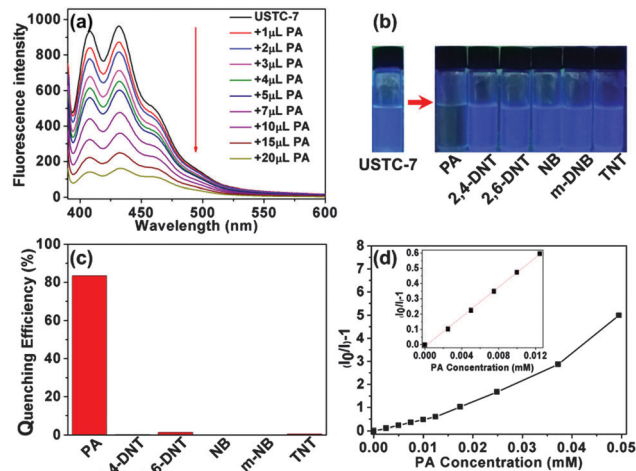


Fig. 3 (a) Fluorescence quenching by incremental addition of 5 mM PA solution to a 2 mL suspension of **USTC-7** in  $CHCl_3$  ( $\lambda_{ex} = 370$  nm); (b) digital photographs of **USTC-7** suspension in the presence of different nitro-explosives under UV light irradiation; (c) comparison of fluorescence quenching efficiencies for various nitro-explosives; (d) Stern–Volmer plot for the fluorescence quenching of **USTC-7** upon addition of PA. Inset: The Stern–Volmer plot at low PA concentrations. The fluorescence intensity at 432 nm was used for analysis.

addition of different nitro-explosives followed by PA into the **USTC-7** suspension. The initial addition of different analytes showed negligible intensity quenching but effective quenching was observed after the addition of the PA solution (Fig. S15–S19, ESI<sup>†</sup>), demonstrating the exceptional selectivity of **USTC-7** for PA.

To gain better insight into the extraordinary PA-sensing ability of **USTC-7**, the electronic properties of MOFs and the nitro-explosives were analyzed. The fluorescence quenching mechanism by electron transfer from the conduction band (CB) of MOFs to the LUMOs of the electron-deficient nitro analytes has been well established.<sup>15</sup> Generally, the CB of electron-rich MOFs is higher than the LUMO energies of nitro analytes and the transfer of excited electrons from the CB of MOFs to the LUMOs of nitro analytes results in fluorescence quenching (Fig. S20, ESI<sup>†</sup>). As the LUMO energy gets lower, the electron accepting efficiency of the nitro analytes and fluorescence quenching become higher. The selective fluorescence quenching by PA is in good agreement with its lower LUMO energy than other nitro analytes (Fig. S21 and Table S5, ESI<sup>†</sup>). The disagreement between fluorescence quenching for other nitro analytes except PA and their LUMO energy trend could be ascribed to other quenching mechanisms associated with electron transfer, such as resonance energy transfer (RET), which is usually responsible for such a quenching response.<sup>8e,f</sup> The effectiveness of the energy transfer significantly relies on the overlap extent between the emission spectrum of the fluorophore and the absorption spectrum of the analyte. The absorption spectrum for PA exhibits a massive overlap with the emission of **USTC-7** (Fig. S22, ESI<sup>†</sup>), in sharp contrast to other nitro analytes without overlap there, which clearly suggests that both electron- and energy-transfer mechanisms are present for fluorescence quenching by PA, while only electron transfer exists for other nitro analytes. In addition, there might be electrostatic interactions between PA molecules and the nitrogen atoms of the ligands



involved in **USTC-7**.<sup>8e</sup> As a result of the combined processes of electron-transfer, energy-transfer and electrostatic interactions between PA and nitrogen atoms of the ligands, the quenching efficiency of PA is significantly enhanced, magnifying the limits of both selectivity and sensitivity.

In conclusion, on the basis of the organic ligand involving both carboxylate and tetrazole groups, an exceptionally stable Zn(II)-MOF, **USTC-7**, in both pH = 2–12 aqueous solution and diverse boiling solvents, has been rationally designed and synthesized, directed by HSAB coordination theory. Remarkably, **USTC-7** exhibits a highly selective and sensitive fluorescence detection of PA, the quenching mechanism of which might be due to the combined processes of electron-transfer, energy-transfer and electrostatic interactions between PA and nitrogen atoms of the ligands. A research endeavor toward the rational synthesis of stable functional MOFs is ongoing in our laboratory. A newly published study reporting a part of similar results came to our attention during the proof stage.<sup>16</sup>

This work was supported by the NSFC (21371162, 51301159 and 21521001), the 973 program (2014CB931803), the Research Fund for the Doctoral Program of Higher Education of China (20133402120020), the State Key Lab of Materials-Oriented Chemical Engineering (KL15-02), the Recruitment Program of Global Youth Experts and the Fundamental Research Funds for the Central Universities (WK2060190026, WK2060190065).

## Notes and references

- (a) J. R. Long and O. M. Yaghi, *Chem. Soc. Rev.*, 2009, **38**, 1213; (b) H.-C. Zhou, R. J. Long and O. M. Yaghi, *Chem. Rev.*, 2012, **112**, 673; (c) H.-C. Zhou and S. Kitagawa, *Chem. Soc. Rev.*, 2014, **43**, 5415.
- (a) J.-R. Li, J. Sculley and H.-C. Zhou, *Chem. Rev.*, 2012, **112**, 869; (b) Y. Peng, V. Krungleviciute, I. Eryazici, J. T. Hupp, O. K. Farha and T. Yildirim, *J. Am. Chem. Soc.*, 2013, **135**, 11887; (c) Z. Wang and S. M. Cohen, *Chem. Soc. Rev.*, 2009, **38**, 1315; (d) J. Pang, F. Jiang, M. Wu, C. Liu, K. Su, W. Lu, D. Yuan and M. Hong, *Nat. Commun.*, 2015, **6**, 7575; (e) B. Chen, S. Xiang and G. Qian, *Acc. Chem. Res.*, 2010, **43**, 1115; (f) H.-X. Zhang, M. Liu, T. Wen and J. Zhang, *Coord. Chem. Rev.*, 2016, **307**, 255.
- (a) R.-B. Lin, F. Li, S.-Y. Liu, X.-L. Qi, J.-P. Zhang and X.-M. Chen, *Angew. Chem., Int. Ed.*, 2013, **52**, 13429; (b) P. Horcajada, C. Serre, M. Vallet-Regí, M. Sebban, F. Taulelle and G. Férey, *Angew. Chem., Int. Ed.*, 2006, **45**, 5974; (c) H. Kitagawa, *Nat. Chem.*, 2009, **1**, 689; (d) B. J. Burnett, P. M. Barron, C. Hu and W. Choe, *J. Am. Chem. Soc.*, 2011, **133**, 9984.
- (a) D. Farrusseng, S. Aguado and C. Pinel, *Angew. Chem., Int. Ed.*, 2009, **48**, 7502; (b) L. Ma, C. Abney and W. Lin, *Chem. Soc. Rev.*, 2009, **38**, 1248; (c) H.-Q. Xu, J. Hu, D. Wang, Z. Li, Q. Zhang, Y. Luo, S.-H. Yu and H.-L. Jiang, *J. Am. Chem. Soc.*, 2015, **137**, 13440; (d) J. Liu, L. Chen, H. Cui, J. Zhang, L. Zhang and C.-Y. Su, *Chem. Soc. Rev.*, 2014, **43**, 6011; (e) J. Gascon, A. Corma, F. Kapteijn and F. X. Llabrés i Xamena, *ACS Catal.*, 2014, **4**, 361; (f) H.-L. Jiang and Q. Xu, *Chem. Commun.*, 2011, **47**, 3351; (g) G. Huang, Y.-Z. Chen and H.-L. Jiang, *Acta Chim. Sinica*, 2016, **74**, 113.
- (a) T. Devic and C. Serre, *Chem. Soc. Rev.*, 2014, **43**, 6097; (b) N. C. Burtch, H. Jasuja and K. S. Walton, *Chem. Rev.*, 2014, **114**, 10575; (c) D. Feng, Z.-Y. Gu, J.-R. Li, H.-L. Jiang, Z. Wei and H.-C. Zhou, *Angew. Chem., Int. Ed.*, 2012, **51**, 10307; (d) H.-L. Jiang, D. Feng, K. Wang, Z.-Y. Gu, Z. Wei, Y.-P. Chen and H.-C. Zhou, *J. Am. Chem. Soc.*, 2013, **135**, 13934; (e) A. J. Howarth, Y. Liu, P. Li, T. C. Wang, J. T. Hupp and O. K. Farha, *Nat. Rev. Mater.*, 2016, DOI: 10.1038/natrevmats.2015.18.
- (a) Y. Cui, Y. Yue, G. Qian and B. Chen, *Chem. Rev.*, 2012, **112**, 1126; (b) L. E. Kreno, K. Leong, O. K. Farha, M. Allendorf, R. P. V. Duyne and J. T. Hupp, *Chem. Rev.*, 2012, **112**, 1105; (c) A. Lan, K. Li, H. Wu, D. H. Olson, T. J. Emge, W. Ki, M. Hong and J. Li, *Angew. Chem., Int. Ed.*, 2009, **48**, 2334; (d) Z. Hu, B. J. Deibert and J. Li, *Chem. Soc. Rev.*, 2014, **43**, 5815.
- (a) J. Ye, L. Zhao, R. F. Bogale, Y. Gao, X. Wang, X. Qian, S. Guo, J. Zhao and G. Ning, *Chem. – Eur. J.*, 2015, **21**, 2029; (b) K. M. Wollin and H. H. Dieter, *Arch. Environ. Contam. Toxicol.*, 2005, **49**, 18.
- (a) S. Sanda, S. Parshamoni, S. Biswas and S. Konar, *Chem. Commun.*, 2015, **51**, 6576; (b) L.-H. Cao, F. Shi, W.-M. Zhang, S.-Q. Zang and T. C. W. Mak, *Chem. – Eur. J.*, 2015, **21**, 15705; (c) D. K. Singha, S. Bhattachary, P. Majee, S. K. Mondal, M. Kumara and P. Mahata, *J. Mater. Chem. A*, 2014, **2**, 20908; (d) Z.-Q. Shi, Z.-J. Guo and H.-G. Zheng, *Chem. Commun.*, 2015, **51**, 8300; (e) S. S. Nagarkar, B. Joarder, A. K. Chaudhari, S. Mukherjee and S. K. Ghosh, *Angew. Chem., Int. Ed.*, 2013, **52**, 2881; (f) S. S. Nagarkar, A. V. Desai and S. K. Ghosh, *Chem. Commun.*, 2014, **50**, 8915; (g) B. Gole, A. K. Bar and P. S. Mukherjee, *Chem. – Eur. J.*, 2014, **20**, 2276; (h) S.-R. Zhang, D.-Y. Du, J.-S. Qin, S.-J. Bao, S.-L. Li, W.-W. He, Y.-Q. Lan, P. Shen and Z.-M. Su, *Chem. – Eur. J.*, 2014, **20**, 3589; (i) Y.-N. Gong, Y.-L. Huang, L. Jiang and T.-B. Lu, *Inorg. Chem.*, 2014, **53**, 9457.
- (a) Y. Lu and B. Yan, *Chem. Commun.*, 2014, **50**, 13323; (b) F.-Y. Yi, Y. Wang, J.-P. Li, D. Wu, Y.-Q. Lan and Z.-M. Sun, *Mater. Horiz.*, 2015, **2**, 245; (c) A. Mallick, B. Garai, M. A. Addicoat, P. S. Petkov, T. Heine and R. Banerjee, *Chem. Sci.*, 2015, **6**, 1420.
- (a) V. Colombo, S. Galli, H. J. Choi, G. D. Han, A. Maspero, G. Palmisano, N. Masciocchic and J. R. Long, *Chem. Sci.*, 2011, **2**, 1311; (b) J. Duan, M. Higuchi, S. Horike, M. L. Foo, K. P. Rao, Y. Inubushi, T. Fukushima and S. Kitagawa, *Adv. Funct. Mater.*, 2013, **23**, 3525; (c) J. Duan, M. Higuchi, R. Krishna, T. Kiyonaga, Y. Tsutsumi, Y. Sato, Y. Kubota, M. Takatae and S. Kitagawa, *Chem. Sci.*, 2014, **5**, 660; (d) Y.-N. Gong, T. Ouyang, C.-T. He and T.-B. Lu, *Chem. Sci.*, 2016, **7**, 1070; (e) J. Dong, P. Cui, P.-F. Shi, P. Cheng and B. Zhao, *J. Am. Chem. Soc.*, 2015, **137**, 15988; (f) J. Cui, Y. Li, Z. Guo and H. Zheng, *Chem. Commun.*, 2013, **49**, 555; (g) H.-R. Fu, F. Wang and J. Zhang, *Dalton Trans.*, 2015, **44**, 2893.
- (a) K.-J. Chen, R.-B. Lin, P.-Q. Liao, C.-T. He, J.-B. Lin, W. Xue, Y.-B. Zhang, J.-P. Zhang and X.-M. Chen, *Cryst. Growth Des.*, 2013, **13**, 2118; (b) H.-Y. Liu, J.-F. Ma, Y.-Y. Liu and J. Yang, *CrystEngComm*, 2013, **15**, 2699.
- A. L. Spek, *J. Appl. Crystallogr.*, 2003, **36**, 7.
- (a) D. N. Dybtsev, H. Chun, S. H. Yoon, D. Kim and K. Kim, *J. Am. Chem. Soc.*, 2004, **126**, 32; (b) P. Li, Y. He, J. Guang, L. Weng, J. C.-G. Zhao, S. Xiang and B. Chen, *J. Am. Chem. Soc.*, 2014, **136**, 547.
- (a) M. D. Allendorf, C. A. Bauer, R. K. Bhakta and R. J. T. Houk, *Chem. Soc. Rev.*, 2009, **38**, 1330; (b) J. Heine and K. Müller-Buschbaum, *Chem. Soc. Rev.*, 2013, **42**, 9232.
- (a) S. J. Toal and W. C. Troglor, *J. Mater. Chem.*, 2006, **16**, 2871; (b) S. Pramanik, C. Zheng, X. Zhang, T. J. Emge and J. Li, *J. Am. Chem. Soc.*, 2011, **133**, 4153.
- X. Wang, M. Xue, G. Wu, Y. Pan and S. Qiu, *Inorg. Chem. Commun.*, 2016, **64**, 31.